Star-Sensor-Based Satellite Attitude/Attitude Rate Estimator

Eliezer Gai,* Kevin Daly,† James Harrison,‡ and Linda Lemos§
The Charles Stark Draper Laboratory Inc., Cambridge, Massachusetts

Recent advancements in star sensor technology suggest that implementations of spacecraft on-orbit attitude determination and control systems based solely on star sensor measurements may soon become practical. This paper defines the requirements such applications impose on the star sensors and the algorithms used to estimate attitude and attitude rate. A practical filter implementation is described. Its open-loop performance is evaluated, and simulation results are presented which suggest that performance consistent with a broad class of spacecraft applications is indeed achievable.

I. Introduction

HISTORICALLY, sensitivity and bandwidth limitations of available star sensors have precluded their use as a primary sensor for on-orbit attitude rate determination. As a result, most practical implementations of satellite attitude determination and control systems have relied primarily on gyroscopes for attitude and attitude rate determination, employing optical measurements (from star sensors, sun sensors, or Earth sensors) when necessary to update the gyro drift estimates.[1-3] The technology for such systems is relatively mature, and several operational spacecraft use stellar-inertial systems as a primary high-precision attitude reference.[4]

Recent advancements in star sensor technology,[5] however, permit a significant increase in both the sensitivity and bandwidth of the stellar information available for on-orbit attitude rate determination. Key features of such sensors include wide field of view (typically 8 deg × 8 deg), high sensitivity (approximately sixth magnitude detection threshold), and low noise (10-20 μrad noise equivalent angle) at a 10-Hz iteration rate.[5] These advancements make it possible to consider practical implementations of on-orbit attitude determination and control systems based solely on star sensor measurements. Of particular interest are star tracker developments based upon charge transfer device (CCD or CID) technologies which suggest performance levels of approximately 10 μrad at 10-Hz update rates.

The gyroless attitude determination and control systems discussed here are most appropriate for spacecraft with low attitude dynamics. Several of the missions for which such spacecraft are required are meteorology, Earth resources, and communications. Among the many attitude control techniques that might be considered for such spacecraft, three-axis-stabilized zero-momentum-bias designs have been found to be appropriate for several high-accuracy missions.[6] In these designs, independent control may be implemented about the principal axes to supplement the system's inherent neutral stability. In zero-momentum designs, the gyroscopic stiffness present in biased-momentum systems (e.g., gyrostats) is sacrificed to permit high bandwidth control about all three spacecraft axes. For these systems, attitude rate information in a bandwidth of approximately 0.5 Hz is required to provide adequate stability. This paper, in conjunction with Ref. 7, describes the design and evaluation of a star-sensor-based attitude determination and control system for these applications.

This paper focuses on the development of a practical filter implementation for estimating attitude and attitude rate based solely on star sensor measurements. The results presented are the *open-loop* performance of the attitude/attitude rate estimators relative to the requirements discussed above. An application of this estimator is described in Ref. 7, which defines the companion controller and documents the closed-loop performance of the attitude determination and control system. The two papers are complementary and overlap only to the extent required to make them self-contained.

The remainder of this paper is divided into three sections. Section II describes the derivation of the filter equations. A six-state extended Kalman filter which incorporates line-of-sight measurements from two skewed star sensors is used to obtain estimates of the spacecraft's attitude and attitude rate. The implementation of this filter, the open-loop evaluation of its steady-state performance, and the sensitivity of its performance to variations in key design parameters are discussed in Sec. III. A brief summary of the authors' conclusions is presented in Sec. IV.

II. Filter Derivation

The equations required for onboard estimation of the spacecraft attitude and attitude rate are derived in this section. The system state vector is defined, and the propagation equations are derived. Another state, referred to as the filter state, is defined to include the errors in the attitude and attitude rate. These errors are estimated using a Kalman filter updated by star sensor measurements. The estimates obtained by the filter are used to improve the system state. Figure 1 is helpful in relating some of the variables that are defined.

A. The System State Vector

The system state vector, x, is a seven-dimensional vector

$$x^T = (q^T, \omega_d^T) \tag{1}$$

where the quaternion q defines the transformation from the body to the inertial frame and ω_d is the rate disturbance expressed in body coordinates.

The nonlinear state equation for the attitude quaternion is given by

$$\dot{q} = \tfrac{1}{2} q (\omega_{\text{nom}} + \omega_d), \qquad q(0) = q_0 \tag{2}$$

where ω_{nom} and ω_d are to be interpreted as quaternions of the form

$$\omega_{\text{nom}}^T = (0, \omega_{\text{nom}}^T) \tag{3}$$

$$\omega_d^T = (0, \omega_d^T) \tag{4}$$

Received Jan. 18, 1983; revision received Nov. 14, 1984.

*Section Chief, Integrated Systems and Controls Division.
†Currently with Odetics Inc., Anaheim Calif.
‡Staff Engineer.
§Currently with DEC Inc., Maynard, Mass.

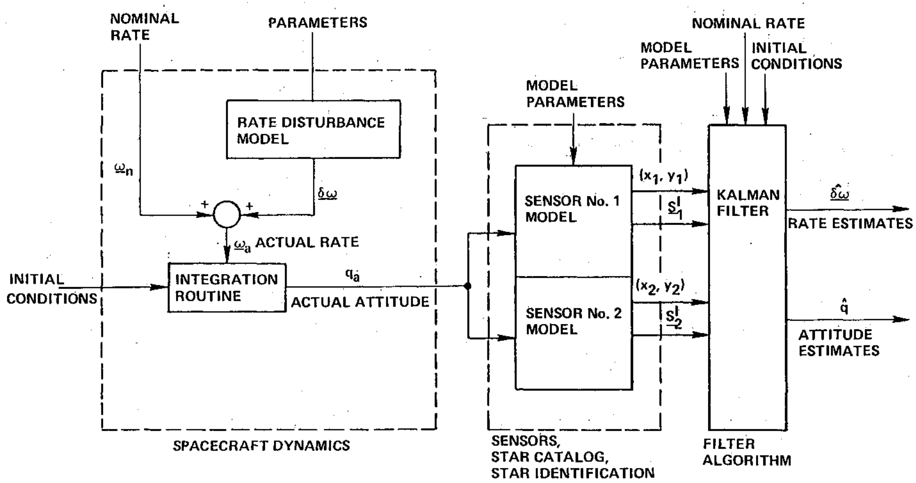

Fig. 1 Software organization.

The vector ω_{nom} is the nominal spacecraft attitude rate expressed in body coordinates.

The rate disturbance ω_d represents the disturbance due to torques produced by the closed-loop control activity. Since the bandwidth of the control system is approximately an order of magnitude smaller than the measurement bandwidth, this low-frequency disturbance can be modeled as a first-order Gauss-Markov process.

$$\dot{\omega}_d = (1/\tau)\omega_d + \nu_d, \qquad \omega_d(0) = 0 \tag{5}$$

where ν_d is a zero-mean white Gaussian random vector with the covariance matrix

$$E[\nu_d(t_i)\nu_d^T(t_j)] = \sigma_d^2 I_3 \delta_{ij} \tag{6}$$

The state estimate is propagated between update times according to the state equations given in Eqs. (2) and (5). The nonlinear equation for the attitude quaternion is integrated using a fourth-order Runge-Kutta method, while the rate disturbance is propagated using the state transition matrix.

B. The Filter State Vector

An extended Kalman filter is used with line-of-sight measurements from two skewed state sensors to obtain corrections to the current attitude and rate estimates. The six-dimensional filter state vector, $\boldsymbol{\delta x}$, is given by

$$\boldsymbol{\delta x}^T = (\boldsymbol{\delta q}^T, \boldsymbol{\delta\omega}^T) \tag{7}$$

where $\boldsymbol{\delta\omega}$ is the rate error vector and $\boldsymbol{\delta q}$ the vector part of the attitude error quaternion. Both of these errors will now be defined.

The attitude error vector $\boldsymbol{\delta q}$ can be defined as follows. Let

$$q_t = \delta q \hat{q} \tag{8}$$

where q_t is the true attitude quaternion, $\hat{q}$ the current attitude quaternion estimate, and

$$\delta q = \begin{bmatrix} \sqrt{1 - |\boldsymbol{\delta q}|^2} \\ \boldsymbol{\delta q} \end{bmatrix} \tag{9}$$

The state equation for $\boldsymbol{\delta q}$ can be obtained by substituting Eq. (8) into the equation

$$\dot{q}_t = \tfrac{1}{2} q_t \omega_t \tag{10}$$

where

$$\omega_t = (0, \boldsymbol{\omega}_t)$$

$$\boldsymbol{\omega}_t = \boldsymbol{\omega}_{\text{nom}} + \hat{\boldsymbol{\omega}}_d + \boldsymbol{\delta\omega} \tag{11}$$

The result is

$$\delta\dot{q} = \tfrac{1}{2}\delta q(\hat{q}\delta\omega\hat{q}^*) \tag{12}$$

where $\hat{q}^*$ is the conjugate transpose of $\hat{q}$. Let $\hat{T}_B^I$ represent the estimate of the body to inertial transformation matrix. Then

$$\hat{q}\delta\omega\hat{q}^* = \begin{pmatrix} 0 \\ \hat{T}_B^I \boldsymbol{\delta\omega} \end{pmatrix} \tag{13}$$

Considering only the dynamics of the vector portion of $\boldsymbol{\delta q}$, the resulting nonlinear equation is

$$\boldsymbol{\delta\dot{q}} = \tfrac{1}{2}[I + [\boldsymbol{\delta q}x]]\hat{T}_B^I \boldsymbol{\delta\omega} \tag{14}$$

where $[\boldsymbol{\delta q}x]$ is a skew-symmetric matrix with elements defined by $\boldsymbol{\delta q}$. The corresponding linear state equation for $\boldsymbol{\delta q}$ is

$$\boldsymbol{\delta\dot{q}} = \tfrac{1}{2}\hat{T}_B^I \boldsymbol{\delta\omega}, \qquad \boldsymbol{\delta q}(0) = 0 \tag{15}$$

[It should be noted that this equation differs from Eq. (135) in Ref. 3. However, both equations are correct and the difference is due to the different definition of $\boldsymbol{\delta q}$.]

The rate error (in body coordinates) is defined as

$$\boldsymbol{\delta\omega} = \boldsymbol{\omega}_d - \hat{\boldsymbol{\omega}}_d \tag{16}$$

and is modeled as a first-order Gauss-Markov process

$$\boldsymbol{\delta\dot{\omega}} = -(1/\tau)\boldsymbol{\delta\omega} + \boldsymbol{\nu}, \qquad \boldsymbol{\delta\omega}(0) = 0 \tag{17}$$

where

$$E[\boldsymbol{\nu}(t_i)\boldsymbol{\nu}^T(t_j)] = \sigma_\nu^2 I_3 \delta_{ij} \tag{18}$$

In summary, the state equation for the filter state vector $\boldsymbol{\delta x}$ is given by

$$\boldsymbol{\delta\dot{x}} = F\boldsymbol{\delta x} + G\boldsymbol{\nu}, \qquad \boldsymbol{\delta x}(0) = 0 \tag{19}$$

where

$$F = \left[\begin{array}{c|c} 0_3 & \tfrac{1}{2}\hat{T}_I^B \\ \hline 0_3 & 1/\tau I_3 \end{array}\right] \tag{20}$$

$$G = \left[\begin{array}{c} 0_3 \\ \hline I_3 \end{array}\right] \tag{21}$$

The error covariance matrix P is propagated using

$$P(t_{n+1}) = \phi(t_{n+1}, t_n)P(t_n)\phi^T(t_{n+1}, t_n) + Q(t_n) \tag{22}$$

A closed-form solution for the state transition matrix ϕ can be obtained for the state equation given in Eq. (19), where it is assumed that F is constant in the interval ΔT from t_n to t_{n+1}

$$\Phi(t_{n+1},t_n) = \left[\begin{array}{c|c} I_3 & (\tau/2)(1-e^{-\Delta T/\tau})\hat{T}^I_B(t_n) \\ \hline 0_3 & e^{-\Delta T/\tau}I_3 \end{array}\right] \tag{23}$$

The discrete process noise covariance matrix $Q(t_n)$ is given by[8]

$$Q(t_n) = \sigma_\nu^2 \left[\begin{array}{c|c} k_1 I_3 & k_2 \hat{T}^I_B(t_n) \\ \hline k_2 \hat{T}^B_I(t_n) & k_3 I_3 \end{array}\right] \tag{24}$$

$$k_1 = (\tau^2/4)[\Delta T - 2\tau(1-e^{-\Delta T/\tau}) + (\tau/2)(1-e^{-2\Delta T/\tau})] \tag{25}$$

$$k_2 = (\tau^2/4)(1-e^{-\Delta T/\tau})^2 \tag{26}$$

$$k_3 = (\tau/2)(1-e^{-2\Delta T/\tau}) \tag{27}$$

C. The Attitude Measurement Equation

The measurements used to provide attitude information are obtained from a star sensor whose optical axis lies along the z_s axis in the sensor frame defined by (x_s,y_s,z_s). The physical measurements are the two coordinates of the star image in the x_s-y_s plane. Let the true star image (without sensor noise) be designated by (p_x,p_y). The unit vector

$$\ell = y/|y| \tag{28}$$

where

$$y^T = (p_x,p_y,f) \tag{29}$$

and f designates the focal length of the optics defines the true line of sight to the star in the sensor frame. The line of sight ℓ is related to the inertial line of sight S^I which is available from a star catalog by two coordinate system transformations

$$\ell = T^S_B T^B_I S^I \tag{30}$$

where T^B_I is the inertial-to-body transformation and T^S_B the body-to-sensor frame transformation.

The apparent line of sight ℓ_A is obtained by adding measurement noise to Eq. (28). Thus,

$$\ell_A = \frac{1}{\sqrt{p_x^2+p_y^2+f^2}} \begin{bmatrix} p_x+\epsilon_y \\ p_y+\epsilon_y \\ f \end{bmatrix} \tag{31}$$

Note that ϵ_x and ϵ_y were omitted from the denominator since they are small compared to p_x, p_y, and f.

Only two components of the unit vector ℓ_A provide independent information. Therefore, the measurement z_A is defined as

$$z_A = A\ell_A \tag{32}$$

where

$$A = \begin{bmatrix} 1 & 0 & 0 \\ 0 & 1 & 0 \end{bmatrix} \tag{33}$$

Using the expressions for ℓ and ℓ_A given by Eqs. (30) and (31), respectively, the measurement z_A can be rewritten as

$$z_A = A\ell + (\ell_z/f)\epsilon \tag{34}$$

where ℓ_z is the z component of ℓ and

$$\epsilon = (\epsilon_x,\epsilon_y)^T \tag{35}$$

The measurement noise vector ϵ is assumed to be a zero-mean random vector with covariance matrix

$$R_\epsilon = \sigma_\epsilon^2 I_2 \tag{36}$$

Equation (34) is the nonlinear measurement equation used to update the estimate of the spacecraft attitude. Note that this measurement equation requires the identification of the star to compute ℓ from Eq. (30). Equation (34) must be linearized with respect to the filter state variables for use in the Kalman filter algorithm. The measurement sensitivity matrix H_A is defined as

$$H_A(t_n) = \left.\frac{\partial z_A}{\partial \delta x}\right|_{\substack{\delta x = 0 \\ x = \hat{x}}} \tag{37}$$

The (2×6) matrix H_A is given by

$$H_A = [H_{qA}, 0_{2\times 3}] \tag{38}$$

where

$$H_{qA} = 2AT^S_B \hat{T}^B_I [S^I x] \tag{39}$$

D. The Attitude Rate Measurement Equation

The attitude rate error δw in the filter state can be updated in a variety of ways. It is updated indirectly when the attitude error δq is updated since the attitude and attitude rate errors are correlated. This procedure requires star identification, however. A procedure that does not require star identification might be desired if attitude rate updates are to be performed much more frequently than attitude updates. This would significantly reduce the size of the star catalog required for a practical implementation. One procedure that does not require star identification could be developed by accounting for the uncertainty in an unidentified star's location in Eq. (34) in the same way as the uncertainty in an unknown landmark's location is treated in Ref. 9. Another approach would consist of implementing a separate attitude rate measurement equation that does not require star identification. It is this approach that is described in detail in this section.

Let p represent the location of the true star image in the sensor x-y plane and let ϵ be the associated measurement noise. The rate measurement $z_R(t_n)$ is defined in terms of the following back difference:

$$z_R(t_n) = (p_n - p_{n-1}) + (\epsilon_n - \epsilon_{n-1}) \tag{40}$$

Referring to Eqs. (28), (31), and (34), the true star image p can be rewritten as

$$p = A|y|T^S_B T^B_I S^I \tag{41}$$

Substituting Eq. (41) into Eq. (40) yields

$$z_R(t_n) = AT^S_B[|y_n|T^B_I(t_n) - |y_{n-1}|T^B_I(t_{n-1})]S^I + \xi_n \tag{42}$$

where

$$\xi_n \equiv \epsilon_n - \epsilon_{n-1} \tag{43}$$

The error ξ_n as defined by Eq. (43) is correlated in time. In order to uncorrelate the error, the state has to be augmented to include the two successive samples of the sensor random errors ϵ_n and ϵ_{n+1}.[10] With two star sensors, this augmentation means the addition of eight components to the state. However, it has been shown that the elimination of these augmented states did not change the performance of the filter.[11] Therefore, the derivation of the rate equation will be continued without this augmentation.

The explicit dependence of z_R on the inertial line of sight of the star S^I can be eliminated by applying Eqs. (41) and (29) to obtain

$$z_R(t_n) = AT_B^S[I - kT_I^B(t_{n-1})T_B^I(t_n)]T_S^B y_n + \xi_n \tag{44}$$

where

$$k = |y_{n-1}|/|y_n| \tag{45}$$

To express the measurement z_R as an explicit function of the angular rate ω^B, it is assumed that the angular rate is constant across one update interval ΔT. Then the following relation holds:

$$T_I^B(t_n) = e^{-W_{n-1}\Delta T}T_I^B(t_{n-1}) \tag{46}$$

where

$$W_{n-1} \equiv [\omega^B(t_{n-1})x] \tag{47}$$

and

$$\Delta T \equiv t_n - t_{n-1} \tag{48}$$

Substituting Eq. (46) into Eq. (44) yields

$$z_R(t_n) = AT_B^S(I - ke^{W_{n-1}\Delta T})T_S^B y_n + \xi_n \tag{49}$$

This equation requires knowledge of the true star image p. However, if the measurement noise is small, p can be replaced by the actual measurement m_n. In addition, if ΔT is sufficiently small, $e^{W_{n-1}\Delta T}$ can be approximated by

$$e^{W_{n-1}\Delta T} \approx I + (\omega_{n-1}^B x)\Delta T \tag{50}$$

Making these substitutions in Eq. (49) yields the nonlinear attitude rate measurement equation

$$z_R(t_n) = AT_B^S[(1-k)I - k(\omega_{n-1}^B x)\Delta T]T_S^B\begin{bmatrix} m_n \\ f \end{bmatrix} + \xi_n \tag{51}$$

where

$$k = \frac{|m_{n-1}|^2 + f^2}{|m_n|^2 + f^2} \tag{52}$$

This measurement equation must be linearized for use in the filter equations. The rate measurement sensitivity matrix H_R is defined by

$$H_R = [0, H_{\omega R}] \tag{53}$$

where

$$H_{\omega R} = \Delta TAT_B^S\left[\left(T_S^B\begin{bmatrix} m_n \\ f \end{bmatrix}\right)x\right] \tag{54}$$

E. Updating the System State Estimates

At scheduled update times, the available sensor measurements are used to update the filter state δx. This update $\hat{\delta x}^+$ is obtained using the standard extended Kalman filter equations.[8] The vector $\hat{\delta x}^+$ includes the estimates of the attitude errors ($\hat{\delta q}^+$) and rate errors ($\hat{\delta\omega}^+$) as components. These components are used to correct the current estimates of the system state as follows:

$$\hat{q}^+(t_n) = \delta\hat{q}^+(t_n)\hat{q}^-(t_n) \tag{55}$$

where

$$\delta\hat{q}^+(t_n) = \begin{bmatrix} \sqrt{1 - |\hat{\delta q}^+(t_n)|^2} \\ \hat{\delta q}^+(t_n) \end{bmatrix} \tag{56}$$

and

$$\hat{\omega}_d^+(t_n) = \hat{\omega}_d^-(t_n) + \delta\hat{\omega}^+(t_n) \tag{57}$$

After incorporating $\delta\hat{q}^+$ and $\delta\hat{\omega}^+$ into the current attitude and rate estimates, these states are reinitialized to zero, i.e.,

$$\hat{\delta q}^+(t_n) = 0, \qquad \delta\hat{\omega}^+(t_n) = 0 \tag{58}$$

It should be noted that by updating the attitude in the way suggested in this section the singularity problem mentioned in Ref. 3 is avoided.

III. Filter Evaluation

A. Evaluation Criteria

In order to provide attitude and attitude rate data suitable for the active stabilization of a spacecraft on-orbit, the open-loop performance of the estimator must satisfy the following requirements. A high bandwidth estimator is required to minimize the impact of the frequency response of the estimator on the stability of the satellite attitude control system which would typically have a bandwidth of 0.2-0.5 Hz. The estimator must be capable of extracting the rate estimates needed for rate feedback in this control system. This implies that the low-frequency content of the rate estimation errors must be small. Estimation characteristics of primary interest are the mean rate error and the root-mean-square (rms) attitude error. Mean rate errors on the order of 5 μrad/s are desired as well as rms attitude errors consistent with an overall system pointing requirement of 174 μrad (0.01 deg). In addi-

Table 1 Bandwidth and low-frequency phase of transfer functions

Axis	Bandwidth, Hz	Phase lag, deg
Yaw	0.67	1.9
Roll	1.2	0.6
Pitch	0.67	1.9

Table 2 Sensor characteristics

Field of view (FOV)	7.5 deg × 10 deg
Focal length	5 cm
Sensor orientation	No. 1 optical axis rotated 45 deg about the positive roll axis from the negative pitch axis
	No. 2 optical axis rotated −45 deg about the positive roll axis from the positive pitch axis
Data rate	10 Hz
Star availability	1 star in FOV of each sensor
Sensor random noise (σ_ϵ)	10 μrad
Sensor systematic errors	None

Table 3 Nominal filter parameters and initial conditions

Rate disturbance model	
Time constant	6 s
Output variance σ_ν	350 μrad/s
Sensor noise	
Attitude measurement (σ_ϵ)	10 μ rad
Attitude rate measurement (σ_ξ)	14 μrad
Update interval	
Attitude update	10 s
Attitude rate update	0.1 s
Initial filter state vector	$\delta x(t_0) = 0$
Initial error covariance	
Attitude errors	305 μrad
Rate disturbance	1.05 mrad/s

Table 4 Summary of baseline performance

	rms Attitude error, μrad			Mean rate error, μrad/s		
	Yaw	Roll	Pitch	Yaw	Roll	Pitch
Case 1	7.7	5.3	7.7	0.02	−0.03	−0.05
Case 2	40.0	21.0	32.0	84.0	55.0	82.0
Case 3	15.5	11.1	14.5	−1.5	0.8	−2.3

tion, the performance of the estimator must be relatively insensitive to the anticipated variations in both sensor error characteristics and on-orbit dynamic environments.

The open-loop performance of the proposed filter implementation for estimating attitude and attitude rate was evaluated both analytically and in a simulation environment. The evaluation effort focused on three critical issues: the dynamic response of the attitude rate estimator, the open-loop performance of the attitude and rate estimators in a range of disturbance environments, and the estimator's sensitivity to star sensor noise characteristics.

B. Filter Dynamic Response

The dynamic response of the proposed attitude and rate estimator can be evaluated from the transfer function array $T(z)$ which relates the true and estimated angular rates. The associated matrix of steady state gains

$$\underset{z \to 1}{T(z)} = \begin{bmatrix} 9.77\times 10^{-1} & 1.84\times 10^{-3} & 4.32\times 10^{-5} \\ 1.84\times 10^{-3} & 9.89\times 10^{-1} & 1.06\times 10^{-6} \\ 4.17\times 10^{-5} & 5.13\times 10^{-6} & 9.77\times 10^{-1} \end{bmatrix} \tag{59}$$

indicates that there is no significant cross-axis coupling between the true and estimated attitude rates. Therefore, the dynamic response of the rate estimator can be inferred from the dynamic response of the transfer functions on the diagonal of $T(z)$. The bandwidth and low-frequency phase lag associated with these transfer functions are indicated in Table 1. These results indicate that the frequency response of the rate estimator, having a bandwidth greater than 0.5 Hz, will not adversely affect the stability of a satellite's attitude control system.

C. Performance Evaluation

The open-loop performance of the attitude and attitude rate estimator was evaluated in a simulation environment. The organization of the software used for this purpose is depicted in Fig. 1. The parameters in Tables 2 and 3 were used to define nominal conditions.

Since the performance of the estimator is a function of the spacecraft's dynamic environment, its performance was evaluated for rate disturbances ranging up to 5 mrad/s within a 0.5-Hz bandwidth. These disturbances were considered representative for the class of satellites of interest. In each case, estimates were obtained over a period of 2 min by incorporating attitude rate measurements at 0.1-s intervals and attitude measurements at 10-s intervals. In all cases, a constant pitch rate of 1.05 mrad/s was assumed in both the truth model and estimation algorithm. This pitch rate reflects the expected dynamic environment of a low-altitude Earth-oriented satellite. The results are summarized in Table 4 and discussed in the following paragraphs.

Case 1 in Table 4 represents the limiting performance of the baseline system when no rate disturbance is present. The observed estimation errors result primarily from sensor noise. Although the means of the rate errors are small (~0.05 μrad/s), these estimates are relatively "noisy" within the estimator bandwidth, having a standard deviation of approximately 40 μrad/s. The estimates, therefore, have significantly different characteristics from those of body rates directly measured by strapdown gyros. The results reported in Ref. 7, however, indicate that the overall bandwidth reduction introduced by the control system results in satisfactory system performance.

Table 5 Sensitivity of attitude errors to sensor noise

Sensor noise level, μrad, 1 σ	rms Attitude error, μrad		
	Yaw	Roll	Pitch
10	23	17	24
60	217	75	214

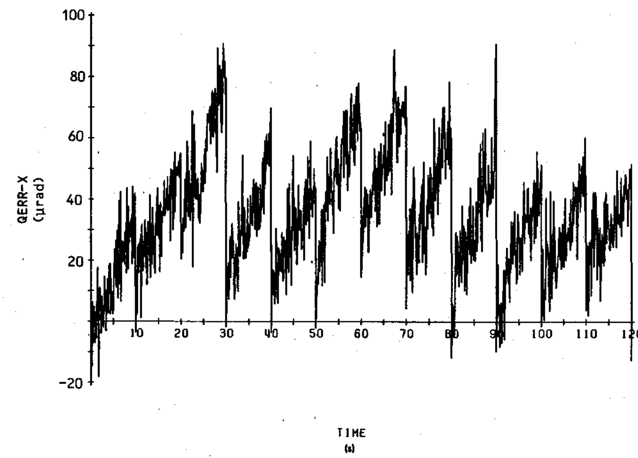

Fig. 2 Yaw axis attitude error for case 2.

Case 2 indicates the estimator performance in the presence of a constant rate disturbance of 5 mrad/s on each axis. This rate error represents a large unmodeled error source for the estimator that results in a significant bias in both the attitude and rate estimates. The attitude bias results in the large rms attitude error (~30 μrad) shown in Table 4. Proportionately smaller biases have been demonstrated for decreased levels of constant rate disturbances. A plot of the resulting yaw axis error over a 2-min period is shown in Fig. 2.

In case 3, the three components of the rate disturbance are modeled as a first-order Gauss-Markov process with a time constant of 6 s and a standard deviation of 0.175 mrad/s. This disturbance is considered by the authors to represent a realistic model of the satellite attitude control system activity for nonmaneuvering Earth-oriented satellites. The performance in this case was well within the performance requirements and, although the mean rate error is somewhat increased from case 1, the standard deviation of the rate estimate (~50 μrad/s) is almost unaffected. The resulting yaw axis error for this case is shown in Fig. 3. The reduced mean attitude error for this case is evident by comparing Fig. 3 with Fig. 2.

D. Estimator Sensitivity

The performance of the estimator was evaluated for star sensors with equivalent random noise standard deviation in the range of 10-60 μrad (~2-12 arcsec). With the exception of this noise term, the baseline parameters defined in Tables 2 and 3 were used in this evaluation. Since sensor noise does not impact the mean of the attitude rate estimation errors (although it does, of course, affect their standard deviations), the rms attitude errors were considered to be the parameter of primary interest for this evaluation. The results of the evaluation are summarized in Table 5.

It is evident from Table 5 that star sensor noise levels of 60 μrad will preclude meeting the system pointing requirement of

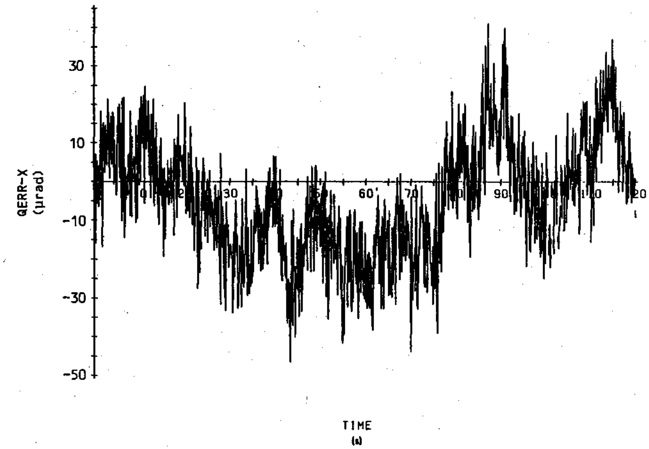

Fig. 3 Yaw axis attitude error for case 3.

175 μrad. The allocation of the pointing error among the estimation, alignment, and control system segments requires a detailed system description, but it is reasonable to require that the estimator not contribute more than one-half of the overall error. Under this assumption, a star sensor with an equivalent random noise standard deviation of 20 μrad or less would be required to meet the overall system pointing requirements.

IV. Conclusions

The results presented herein indicate that advances in star sensor technology now make it possible to derive attitude rate information in a bandwidth adequate to ensure the stability of attitude determination and control systems for a broad class of satellite applications. An extended Kalman filter which can be used on-orbit to estimate attitude and attitude rate from star sensor measurements has been developed. The open-loop performance of this estimator has been shown to be consistent with that which is required for the active stabilization of a satellite. This performance was verified in the presence of realistic vehicle disturbances and uncertainties in the star sensor characteristics. On the basis of the open-loop performance of the attitude and attitude rate estimator described in this paper, the closed-loop performance of a gyroless attitude determination and control system which incorporates the estimator was evaluated in the context of an advanced environmental satellite application. The result of that evaluation are reported in Ref. 7.

References

[1]White, R.L., Adams, M.B., Gai, E., and Grant, F., "Attitude and Orbit Determination Using Stars and Landmarks," *IEEE Transactions on Aerospace and Electronic Systems,* Vol. AES-11, No. 2, March 1975, pp. 195-202.

[2]Sorensen, J.A., Schmidt, S.F., and Goka, T., "Application of Square Root Filtering for Spacecraft Attitude Control," *Journal of Guidance and Control,* Vol. 2, Sept.-Oct. 1979, pp. 426-433.

[3]Lefferts, E.J., Markley, F.L., and Shuster, M.D., "Kalman Filtering for Spacecraft Attitude Estimation," *Journal of Guidance and Control,* Vol. 5, Sept.-Oct. 1982, pp. 417-429.

[4]Hoffman, D.P. and Berkery, E.A., "On-Orbit Experience with the HEAO Attitude Control Subsystem," AIAA Paper 78-1263, Aug. 1978.

[5]Jones, C. and Kollodge, J., "An Advanced Tracker Design for Pointing and Control of Space Vehicle Using the Charge Injection Device," 1982 Rocky Mountain Guidance and Control Conference, Keystone, Colo., 1982.

[6]Phillips, K.J., Schmidt, G.E., and Podgorski, W., "Post-Launch Design and Implementation of a Momentum Bias Attitude Control System," AIAA Paper 79-1720, Aug. 1979.

[7]Podgorski, W.A., Lemos, L.K., Cheng, J., and Daly, K.C., "Gyroless Attitude Determination and Control System for Advanced Environmental Satellites," AIAA Paper 82-1614, Aug. 1982.

[8]Gelb, A., ed., *Applied Optimal Estimation,* MIT Press, Cambridge, Mass., 1974.

[9]Toda, N.F. and Schlee, F.H., "Autonomous Orbital Navigation by Optical Tracking of Unknown Landmarks," *Journal of Spacecraft and Rockets*, Vol. 4, Dec. 1967, pp. 1644-1648.

[10]Daly, K. et al., "Technical Status Review, Satellite Systems Design Study," The Charles Stark Draper Laboratory, Cambridge, Mass., CSDL P-1145, July 1980.

[11]Gai, E. et al., "Technical Status Review, Satellite Systems Design Study, The Charles Stark Draper Laboratory, Cambridge, Mass., CSDL P-1209, Oct. 1980.